

Seasonal variation of water column structure and sediment transport in a mud depo-center off the Zhejiang-Fujian coast in China

Yunhai Li · Lei Qiao · Aijun Wang · Yong Zhang · Jianyong Fang · Jian Chen

Received: 3 March 2012 / Accepted: 24 April 2013 / Published online: 22 May 2013
© Springer-Verlag Berlin Heidelberg 2013

Abstract Two surveys were conducted in December, 2008, and August, 2009, in the mud depo-center off the Zhejiang-Fujian coast (MDZFC) in the inner shelf of East China Sea to depict the seasonal variation of the water column structure and analyze the factors responsible for the variation. The results were also used to discuss the sediment transport process and formation mechanism of the MDZFC. The water column structures varied significantly between the two surveys, with respect to the temperature, salinity, and turbidity. The summer water body, with relatively high temperatures and salinities, was evidently stratified with respect to the temperature, whereas the salinity remained constant throughout the water column. The stratification restricts sediment resuspension and transport. From the north to the south, the temperature in the middle-bottom water layer slightly increased, whereas the salinity remained mostly constant. In winter, the water body, with relatively low temperatures and salinities, was well mixed vertically. The temperature and salinity both increased

from the surface to the bottom toward the east (deep water) and the south. A wedge-shaped water mass, which appears as a coastal upwelling, with relatively low temperature and high salinity in summer and relatively high temperature and high salinity in winter, spread landward along the sea floor, from the sea deeper than 50 m, whereas the extension was relatively stronger in winter. The water turbidity in winter was clearly higher than in summer. In the surface layer, the turbidity was generally greater than 5 FTU in winter and less than 1 FTU in summer. In the bottom layer, the turbidity was much greater than 200 FTU in winter and slightly greater than 50 FTU in summer. Moreover, the turbid water layer close to the sea floor in winter can reach into an area deeper than 50 m with a thickness of over 10 m; however, it was only limited to only 30-m-deep water with a thickness of 5 m in summer. The differences of marine sedimentary environment in the MDZFC were attributed to the seasonal variations of hydrodynamics environment, weather conditions, sediment supplies, and seasonal circulations. The results suggest that winter is the key season for particle transportation and deposition. The bottom turbid layer is the primarily channel of sediment transport, and the upwelling currents and the oceanic front systems play an important role in the sediment deposit processes and the formation of the MDZFC.

Responsible Editor: Andrew James Manning

This article is part of the Topical Collection on the *11th International Conference on Cohesive Sediment Transport*

Y. Li (✉) · A. Wang · J. Fang · J. Chen
Third Institute of Oceanography, State Oceanic Administration,
Xiamen 361005, China
e-mail: liyunhai1980@gmail.com

L. Qiao
Hydrometeorology and Remote Sensing Laboratory,
University of Oklahoma, Norman, OK 73019, USA

Y. Zhang
Qingdao Institute of Marine Geology, Qingdao 266071, China

J. Fang
State Key Laboratory of Marine Geology, Tongji University,
Shanghai 200092, China

Keywords Seasonal variation · Sedimentary environment · The East China Sea · Sediment transport

1 Introduction

Most major rivers (rivers with high sediment and/or water discharge rates) typically develop massive delta depositional systems (such as the delta plain, subaqueous delta, and along-shore clinoform, among others) at their estuaries and along

coast areas, which plays a disproportionately important role in the transportation of dissolved and particulate materials from the terrestrial environments to the coastal ocean. These depositional systems store an abundance of geological information (e.g., the materials flux, the depositional cycles, and their variability, which are influenced by the marine dynamics and climatic changes as well as intense human activities), which act as important media for the study of land–ocean interaction, oceanic mass flux, and biogeochemical cycles (including the global carbon cycle). The sediment supplies and marine dynamic conditions are the two key environmental factors in the formation of these depositional systems (see, e.g., DeMaster et al. 1986; Kuehl et al. 1986, 1997; Allison et al. 2000; Su and Huh 2002; Cattaneo et al. 2003; McKee et al. 2004; Liu et al. 2006, 2007, 2009; Xu et al. 2009, 2012).

The East China Sea (ECS) is a typical river-dominated marginal sea with abundant terrestrial particles supplied by the Yangtze and Yellow Rivers (including the abandoned old Yellow River). The Yangtze River, which is the largest Asian river and third longest river in the world, has provided an annual supply of 240×10^6 t of sediments into the ECS since the high sea-level era (7,000 year BP), of which 47 % are deposited in estuarine subaqueous deltas, 21 % are deposited in near-shore subaqueous deltas, and the remaining 32 % are deposited in the Zhejiang-Fujian coast, forming a mud depo-center off the Zhejiang-Fujian coast (MDZFC; Fig. 1a) (Liu et al. 2006). As a sediment sink, the MDZFC is significantly influenced by the sediment supplies from the Yangtze River and the ECS circulations, both of which display seasonal characteristics. First, the sediment supplies and deposition rates vary seasonally. The sediment discharge in the flood season (May–October) account, for approximately 87 % of the total annual discharge (Xu and Milliman 2009), and the monthly rate of deposition in the Yangtze River estuary is 4.4 cm between June and September. This rate is much larger than the annual average rate of 1.6 cm (McKee et al. 1983; DeMaster et al. 1985), which indicates that a significant fraction of the deposited sediments must be resuspended and transported in the dry season (winter). Second, the flow direction of the ECS coastal current shifts from northward in summer to southward in winter due to the East Asian monsoon (Su 2005), which controls the sediment transport and deposition in the ECS margin. Due to the obstruction of the northward summer monsoon and the related circulations, the sediment discharged from the Yangtze River is generally rapidly deposited in the estuary area in summer. The deposited sediments can be resuspended by extreme storm events and transported southward along the coast in winter (Milliman et al. 1985; Yang et al. 1992; Hu and Yang 2001; Guo et al. 2003; Liu et al. 2006; Xu and Milliman 2009; Xu et al. 2009). The study of the sediment flux in the East China Sea has been widespread, and some consensus have been reached over the past few decades. Additionally, abundant sedimentary

indexes (such as grain size, sedimentary stratum, geochemical elements, and minerals) were successfully applied to reveal the climatic changes, sediment sources, and sedimentary environment in the MDZFC and its surrounding area (see, e.g., Huh and Su 1999; Xu and Milliman 2009; Dong et al. 2011; Li et al. 2010; Liu et al. 2010, 2011). However, the dynamics of the sedimentary processes and their seasonal variations, which form the background for the study the environmental and geological records in the ECS shelf, are rarely mentioned in the previous studies.

Recently, Liu et al. (2006, 2007), Xu (2009) and Xu et al. (2009, 2012) used high-resolution stratigraphic profiles, geochronology records, lithology, and sediment size analysis to study the spatial distribution, temporal evolution, and sediment flux of the ECS inner-shelf mud zone. A primary conceptual model was constructed based on the study results to reveal the hydrodynamic mechanism and the formation of the mud depo-center (Liu et al. 2006, 2007). However, the model was limited and inaccurate due to the absence of seasonal in situ hydrographic observations. In two marine hydrodynamic studies, Lv et al. (2006) and Qiao et al. (2006) combined field observations, SST satellite images and numerical simulations to study the distribution, formation, and variation of the upwelling in the ECS shelf, both in summer and winter. The studies demonstrated that the upwelling, which exists all year round in the ECS shelf, is a fallout of multiple mechanisms, including the circulations, tide, topography, and winds in the region. The upwelling studies acquired significantly innovative realizations and could provide important constraints on the dynamic nature of the MDZFC, even though the sediment transport and deposit effects were not included.

The aims of this study are the following: (1) to depict the seasonal variation of the water column structure in terms of temperature, salinity, and turbidity distributions in the MDZFC based on field data obtained during two surveys conducted during winter and summer, (2) to analyze the factors responsible for the seasonal variations of the water column and geological records, and (3) to discuss the sediment transport process and the formation mechanism of the MDZFC.

2 Surveys and method

2.1 Surveys

Two surveys were conducted on the MDZFC (Fig. 1b). The first survey was conducted from December 5 to 7, 2008, and the second survey was conducted from August 1 to 3, 2009. In the first survey, the measurements were recorded at 25 stations divided into five sections from south to north. The weather was unfavorable because of

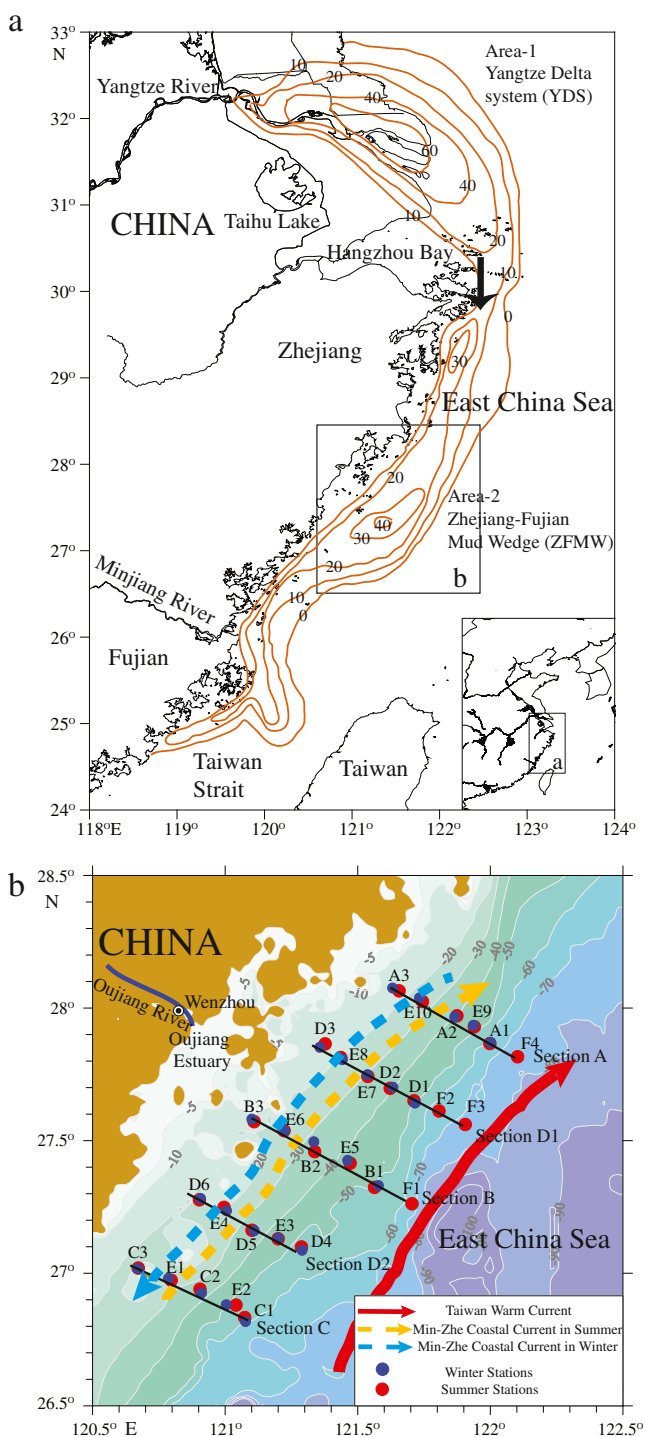


Fig. 1 a Isopach map (in meters) of the Yangtze-derived sediment deposited over the last 7,000 years in the inner shelf of the ECS (after Liu et al. 2006). b Station and survey sections; note that the Min-Zhe Coastal Current flows southward in summer (yellow dotted line) and northward in winter (blue dotted line) controlled by the Asian Monsoons, while the Taiwan Warm Current flows northward all year round (red solid line)

the winter cold storm affect, with wave heights of 2.3–3.5 m and the north wind speed remained higher than 13.0 m/s (data from the Ocean Monitoring and Forecasting Center of the

Zhejiang Providence, www.zjhy.net.cn). In the second survey, the measurements were recorded at 29 stations divided into five sections (same as in the first survey). The weather was calm with the south wind speed less than 10.7 m/s, and wave heights less than 1.6 m (data from the Ocean Monitoring and Forecasting Center of the Zhejiang Providence, www.zjhy.net.cn).

2.2 Method

An SD204 CTD was used to record the water temperature, salinity, depth, and turbidity throughout the water column. Water samples were collected at six different depths during the CTD cast at selected stations. The sampled water layers were at the surface and bottom depths as well as at 0.2, 0.4, 0.6, and 0.8 fraction of the total water depth. The surface water samples were taken using a plastic bucket. The sample volumes ranged from 1,200 to 2,000 ml, depending on the observed turbidity of the water. The water samples were filtered in the laboratory by pumping through pre-weighed double filters with a diameter of 47 mm and a pore diameter of 0.45 μm. The filters were rinsed with distilled water to remove the salt, dried at 40.0 °C, and then weighed using an electronic balance with a precision of 10⁻⁵ g. The weight of the sediment on the upper part of the two filters was corrected by the weight of the lower, empty filter. The units used for the total suspended matter (TSM) were milligrams per liter.

A clear linear correlation was found upon the regression of the TSM data from the 101 water samples with the water turbidity at the same depths (Fig. 2). This results show that

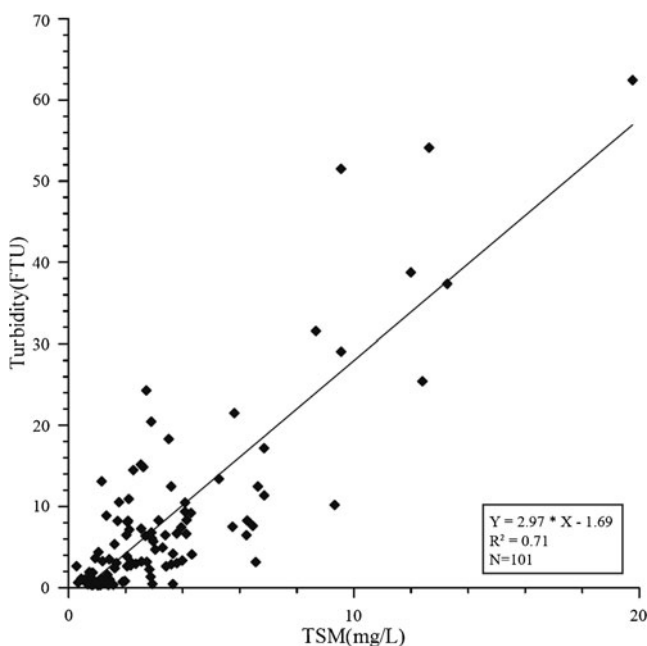


Fig. 2 Relationship between the water turbidity and TSM

the water turbidity can largely account for the continuous variations in the TSM of the water column, as demonstrated in previous studies (Hoshika et al. 2003).

3 Results

3.1 Water temperature, salinity, and turbidity in summer

The spatial pattern of the physical properties of the surface water layer (5 m below the sea surface) and bottom water layer (5 m above the sea floor) during summer are shown in Fig. 3. Toward the deep water, a gradual decrease of the temperature and turbidity and an increase in the salinity demonstrate the standard summer pattern. The physical properties of the surface water, namely, high temperatures

(greater than 28.0 °C), high salinity (greater than 33.5 psu), and low turbidity (less than 1 FTU), are relatively consistent and have minor spatial variations. However, the spatial patterns in the bottom layer show significant seaward change, in which the temperature and turbidity decrease from 25.0 to 18.0 °C and from 50 FTU to 10 FTU, respectively, whereas the salinity increases from 34.0 to 34.5 psu. The maximum gradients occur at the 40–50 m isobath for both the temperature and salinity.

The cross-shelf sections of A, B, and C show a general decrease in the temperature and increases in the salinity and turbidity from the surface to the bottom (Fig. 4). The thermocline occurs at a depth of approximately 10 m, above which the temperature is higher than 27.0 °C and below which the temperature is between 23.0 and 26.0 °C. The water below 50 m is much cooler with temperatures less

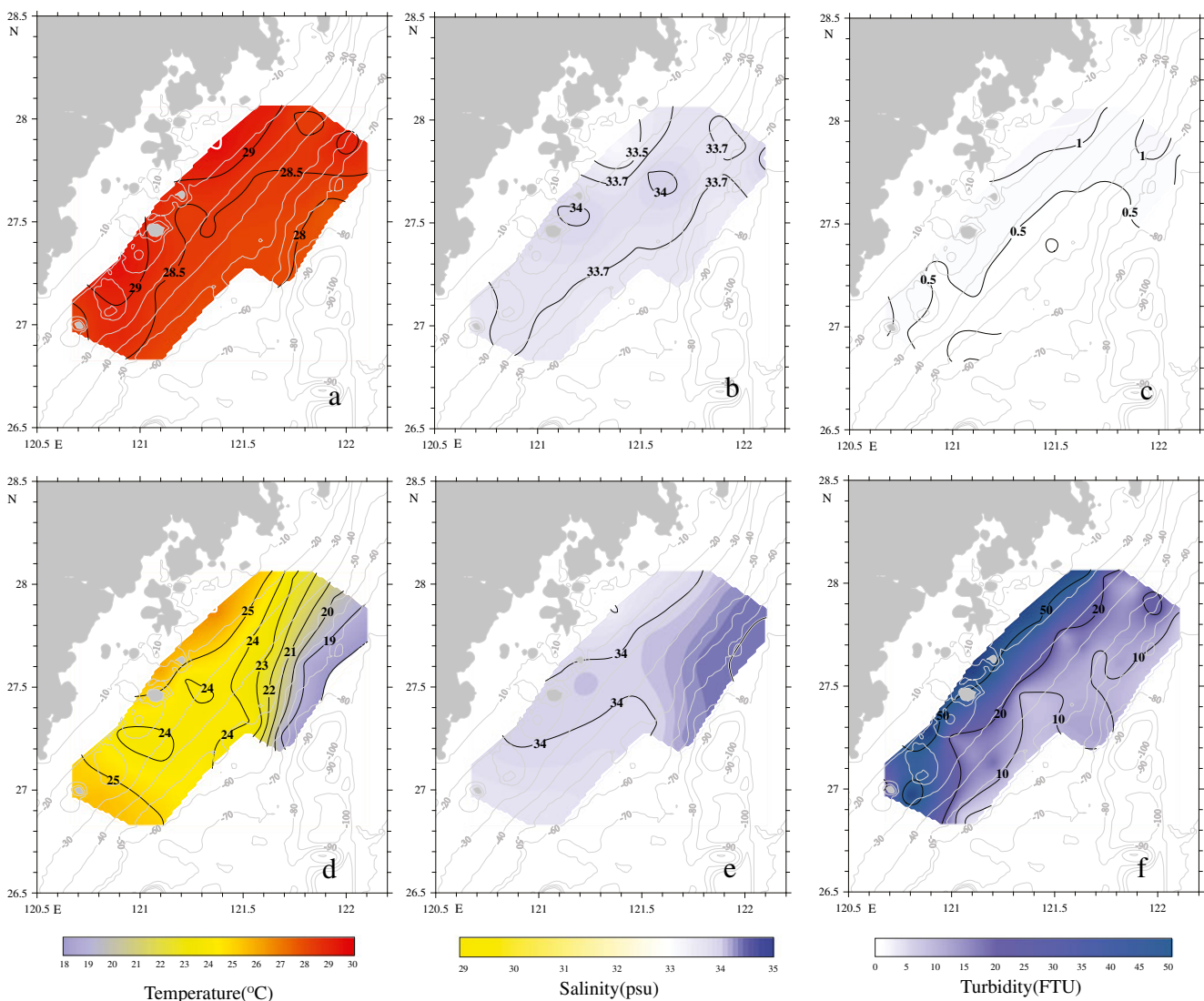


Fig. 3 a Temperature, b salinity, and c turbidity distributions in the surface layer and d temperature, e salinity, and f turbidity distributions in the bottom layer in summer. The bottom turbid layer distributed in

the coastal area and the maximum gradients occur at the 40–50 m isobath for the temperature and salinity

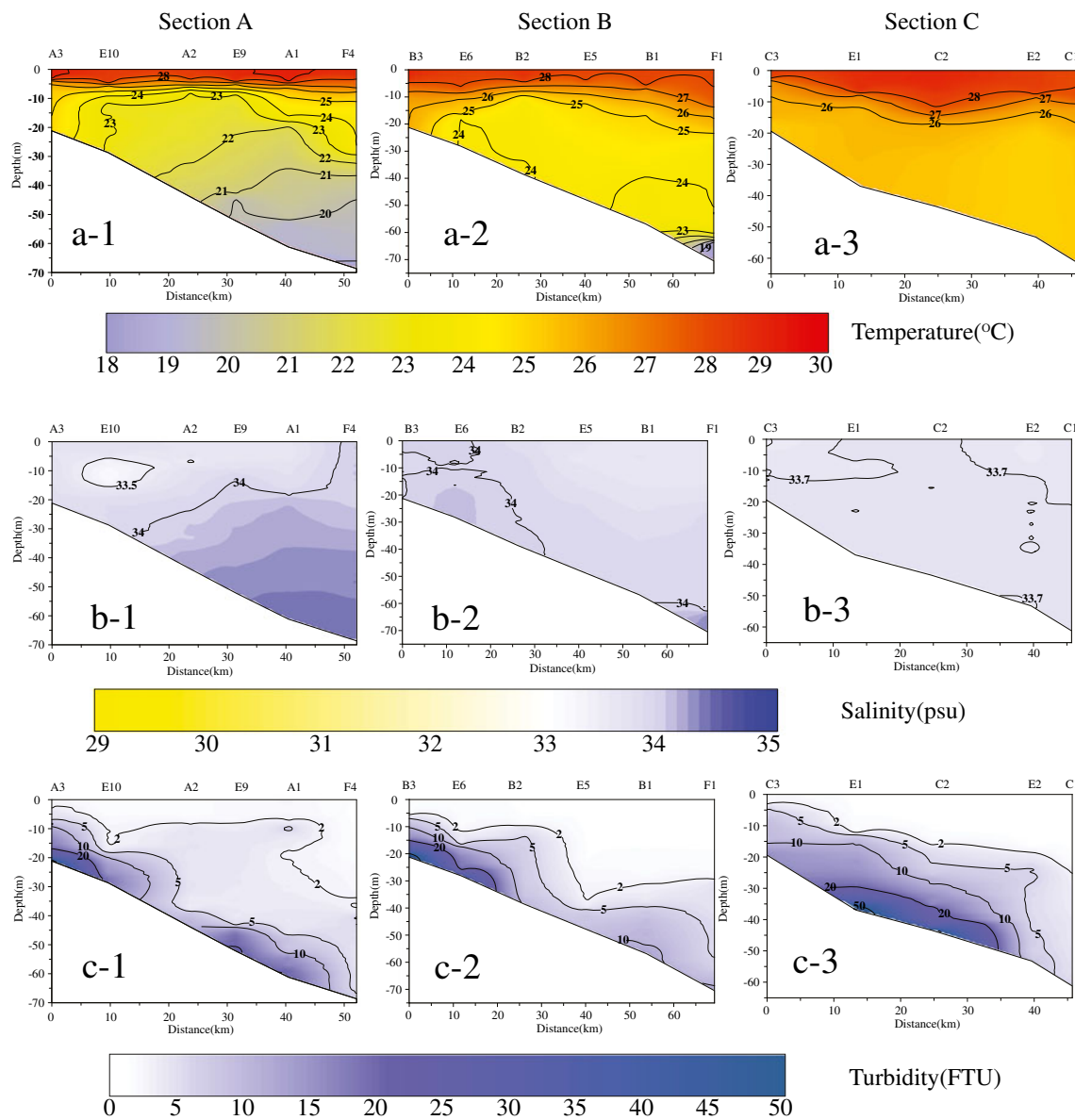


Fig. 4 Temperature, salinity, and turbidity distributions within the sections in summer *a-1* temperature distribution on *section A*; *a-2* temperature distribution in *section B*; *a-3* temperature distribution in *section C*; *b-1* salinity distribution in *section A*; *b-2* salinity distribution in *section B*; *b-3* salinity distribution in *section C*; *c-1* turbidity

distribution in *section A*; *c-2* turbidity distribution in *section B*; and *c-3* turbidity distribution in *section C*. The water column is stratified and the thermocline occurs at a depth of approximately 10 m. Upwelling exists below a water depth of 50 m

than 20.0 °C, which demonstrates a decreasing trend from the north to south. The salinities in the three sections do not vary significantly, and range from 33.5 to 34.5 psu. The cold water that is deeper than 50 m also has a relatively higher salinity (greater than 34.3 psu). The water turbidity increases rapidly when close to the seafloor, which forms the bottom turbid layer. The turbidity in the bottom turbid layer is generally greater than 5 FTU and can reach up to 50 FTU in some place, decreasing toward the deep sea with a shrinking-upward tendency that extends from the north to south. The turbidity is higher in the northern section because it is closer to the estuary of the Yangtze River.

As shown above, the study area is dominated by coastal water with high temperatures, high salinity, and low turbidity, during the summer. The water column is stratified with a thermocline formed at a water depth of 10 m. The salinity is relatively uniform throughout the column without any evidence of stratification. The water mass that is deeper than 50 m is outsourced from the deep-sea, and upwells as a wedge with high salinity and low temperature, with the extension of the deep-sea water increasing from the south to the north. The water turbidity is very low in the upper layer but high enough at the bottom to form the bottom turbid layer. From the north to the south, the water body has

significant variations in temperature, salinity, and turbidity. The upwelling of the deep water, intruded from the Taiwan Warm Current, was toward the north, a location that agrees well with previous studies (Zhu 2003; Lv et al. 2006).

3.2 Water temperature, salinity, and turbidity in winter

The winter spatial pattern of the physical properties of the surface water layer (5 m below the sea surface) and bottom water layer (5 m above the sea floor) are shown in Fig. 5. Toward the deep water, a gradual increase of temperature and salinity and a rapid decrease of turbidity typify the standard winter pattern. In the surface water, the relatively low temperature and low salinity increase toward the east, from less than 14.0 °C to slightly greater than 18.0 °C, and

from less than 27.0 psu to greater than 33.0 psu, respectively. The turbidity decreases toward the southwest, from greater than 50 FTU to less than 2 FTU. In addition to the eastward increase, the temperature and salinity also show southward increases of 0.5–2.0 °C and 1.0–2.0 psu, respectively. The variations in the variables of the bottom water layer are similar to those in the surface layer but with values that are increased by 0.5–1.0 °C, 1.0 psu, and three- to fourfold for the temperature, salinity, and turbidity, respectively. The turbidity, which is generally greater than 20 FTU and can reach a maximum value of 200 FTU, spreads eastwardly to water depths of 40–50 m. The wedge-shaped high-temperature and high-salinity water mass diffuses toward the near-shore environment at water depths greater than 50 m.

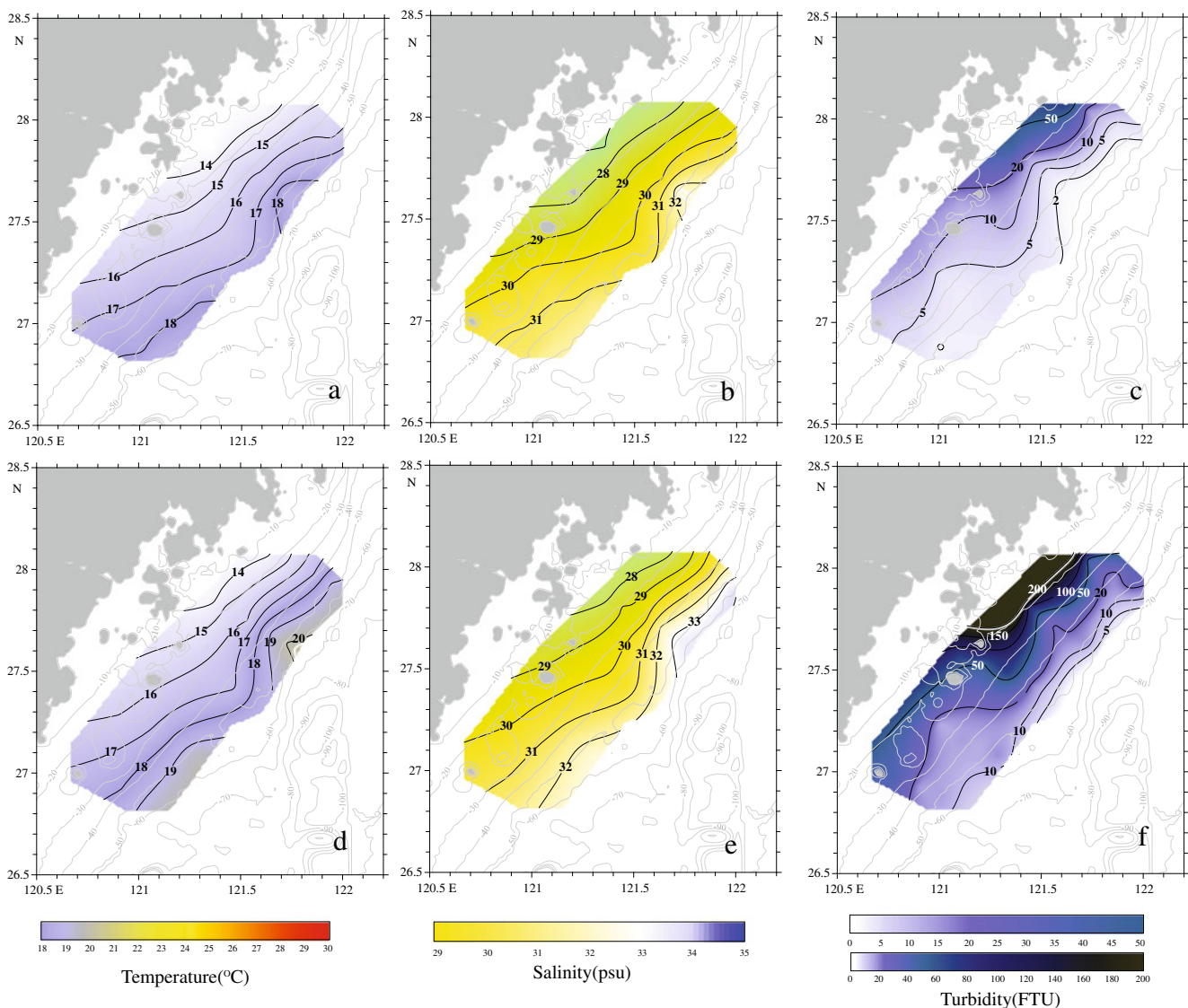


Fig. 5 a Temperature, b salinity, and c turbidity distributions in the surface layer and d temperature, e salinity, and f turbidity distributions in the bottom layer in winter. The bottom turbid layer distributed in the

coastal area and the maximum gradients occur at the 40–50 m isobath for the temperature and salinity

During winter, the sections A, B, and C (Fig. 6) largely show a vertical uniformity in the temperature and salinity due to mixing. The temperature and salinity increase from 14.0 to

20.0 °C and 28.0 to 33.0 psu, respectively, toward the deep water. The turbidity is generally higher than 5 FTU, and the bottom turbid layer is formed below the intermediate water

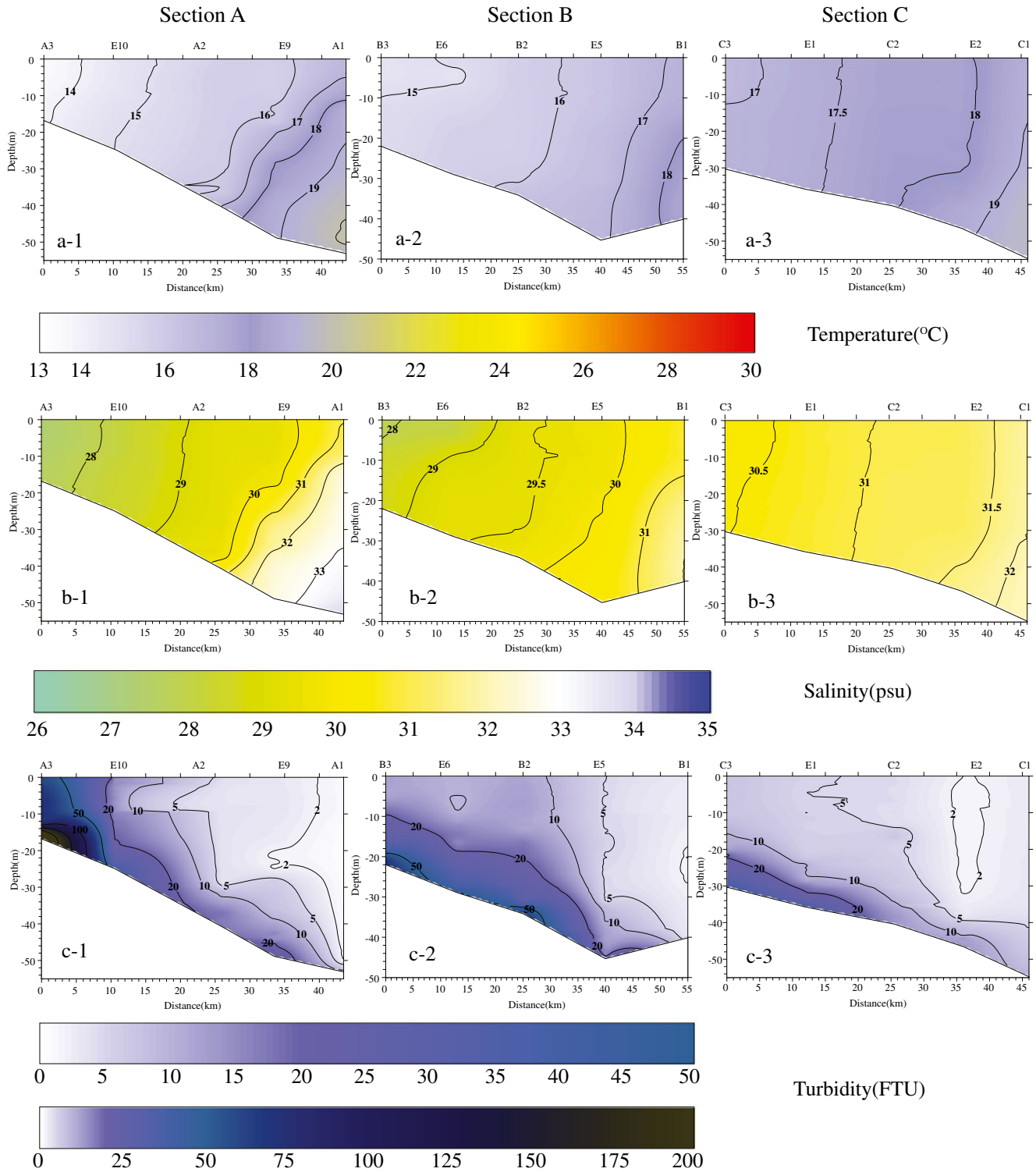


Fig. 6 Temperature, salinity, and turbidity distributions in the sections for winter a-1 temperature distribution in section A; a-2 temperature distribution in section B; a-3 temperature distribution in section C; b-1 salinity distribution in section A; b-2 salinity distribution in section B;

b-3 salinity distribution in section C; c-1 turbidity distribution in section A; c-2 turbidity distribution in section B; c-3 turbidity distribution in section C. The water column was well mixed without a thermocline and upwelling existed below a water depth of 50 m

body, the intensity and depth of which gradually decrease with increasing water depths. From the north to the south, the rise in temperature (by 1.0–3.0 °C) and salinity (by 0.5–2.0 psu) accompany the decrease in the turbidity, both in magnitude and extent, across the three sections. The diffusion of the high-temperature and high-salinity water wedge toward shallow water also decreases southwardly.

The water column in the study area in the winter is primarily controlled by the low-temperature, low-salinity, and high-turbidity coastal currents, and it is vertical well-mixed. The bottom turbid layer spreads upward and becomes less turbid with increasing water depth, despite the fact that the water turbidity of the whole water layer remained very high in the coastal area. From the north to the south, minor increases in the temperature and salinity are seen, along with a gradual decrease in the turbidity because of the settling of the sediments. Relatively warm and salty water upwelled into the shallow water along the sea floor. The upwelling was primarily towards the north, which agrees with observations made in previous studies (Gong et al. 2003; Qiao et al. 2006).

4 Discussions

4.1 Seasonal variations of the water column structure and the factors influencing them

As shown above, the water column structure (temperature and salinity distributions) and suspended particle contents (turbidity distribution) were markedly different in the two surveys (Figs. 3, 4, 5, and 6). In summer, the water structure was stratified, and a thermocline formed approximately 10 m, with high temperatures and salinities, which varied between 20.0 and 28.0 °C and 33.0 and 34.4 psu, respectively (Figs. 3, 4, and 7). In winter, the water body was highly mixed vertically, without any thermo-halocline, with relatively low temperatures and salinities, which varied from 14.0 to 19.0 °C and 28.0 to 33.0 psu, respectively (Figs. 5, 6, and 7). The study area is dominated by coastal water, with the Taiwan Warm Current (TWC) located near the eastern boundary, both in summer and winter. The high temperature and uniform salinity observed during summer indicated that the coastal water and the deeper TWC had originated from the same source (Fig. 7), namely, the Taiwan Strait, as was shown in the previous study (Chen 2009). However, during winter, the coastal water and the deeper TWC originated separately with markedly different characteristics (Fig. 7). The coastal current originated in the north, and carried abundant relatively fresher waters, while the TWC was from the Taiwan Strait in the south, with higher salinities (Su 2005).

The water turbidity in summer, with regards to the content of the suspended particles, is less than 1 FTU and is

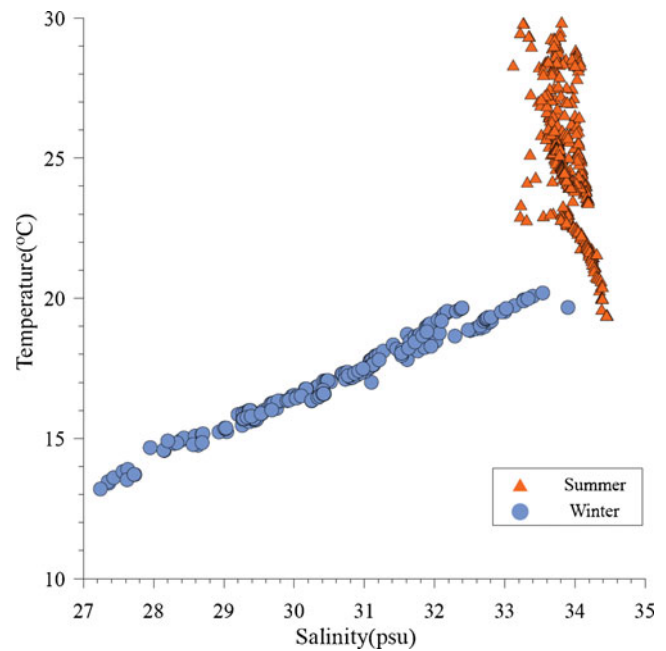


Fig. 7 Temperature/salinity (*T/S*) plots for all the hydrographic stations occupied in summer (*triangle symbols*) and in winter (*closed circles*)

slightly greater than 50 FTU in the surface and bottom layer, respectively. In winter, the turbidities are greater than 5 FTU and 200 FTU in the same layers. Water with turbidities greater than 20 FTU, the turbid water layer, can have a layer depth of up to a maximum value of 10 m. The water can diffuse eastwardly to a water depth of 40 m in winter. However, the same water body is only 5 m deep in summer, reaching a water depth of 30 m. Upwelling water, with relatively low temperatures and high salinities in summer, and high temperatures and high salinities in winter, was observed in the deep water toward the northeast of the study area, which agreed well with the locations observed in the previous studies (Gong et al. 2003; Zhu 2003; Lv et al. 2006; Qiao et al. 2006).

The seasonal variations of the water structures can be largely attributed to the hydrodynamic conditions, weather, and seasonal circulations. The MDZFC is controlled primarily by the coastal currents, which flows from the south to the north during summer, just as the TWC flows to the east. The trend is reversed in winter, the coastal currents flows from the north to the south and opposite to the TWC (Su 2005). In summer, the water body was clearly stratified, with high temperatures due to the warm and calm weather (south wind) and intense solar radiation. The coastal current and the deeper TWC both originated from the Taiwan Strait and displayed similar temperatures and salinities (Su 2005; Chen 2009). In winter, however, the water body was well mixed vertically, with relatively low temperatures due to the cold and stormy weather (north wind). The coastal currents that originate in the north carry abundant fresh water, while the

TWC with relatively high salinity originates from the Taiwan Strait (Su 2005).

The cogenetic coastal waters and the TWC were relatively clean due to lack of runoff input during summer (Su 2005). Moreover, the weak winds and the strong stratification greatly restricted the sediment resuspension. The turbidity was relatively low in the entire water column (Figs. 3 and 4). In contrast, the coastal water, flowing from the north in winter, carried abundant sediments that were discharged and resuspended from the Yangtze River and its ambient estuary. Additionally, the severe winter winds stirred up the water column substantially and induced complete mixing and considerable sediment resuspension. Therefore, the turbidity increased abruptly in the coastal area and was in sharp contrast with the TWC (Figs. 5 and 6). An oceanic front was therefore established between the coastal water and the TWC water due to the significantly different physical properties and flow directions (Chen 2009), especially during winter (Figs. 3 and 5). The perennially northward directed TWC, which restricts the across-shelf transport of suspended particles from the coastal area, intrudes into the coastal water due to the topography and the baroclinic pressure gradient, and forms the upwelling current (Lv et al. 2006; Qiao et al. 2006).

Figure 8 summarized the seasonal variations of the water structure and the responsible factors in a conceptual diagram.

4.2 The seasonal sedimentary processes and their sedimentary records in the MDZFC

The study area, with water depths of less than 60 m, covers the inner mud deposition center of the ECS. The sediments mainly consist of clay silts and are up to 40 m deep in the center of deposition (Fig. 1a) (Liu et al. 2006). Previous studies have suggested that the Yangtze River is the primarily source of the sediments. In summer, the discharged particles, which are dominated by the monsoons and northwardly flowing coastal currents, are seldom transported to the outer shelf and are mostly deposited in the estuary (Liu et al. 2006; Xu et al. 2012). In winter, the monsoon-driven coastal currents flow southward and cause downwelling of the nearshore waters, whereas the northward-flowing TWC causes upwelling (Su 2005). With these two vertical circulation cells in place, the resuspended sediments can then be transported southward again along the coast during extreme storm events (Liu et al. 2006). The oceanic front between the coastal water and the TWC acts as a water barrier to obstruct the sediment transport from the coast to the outer shelf (Hu and Yang 2001; Chen 2009). Therefore, the particle-rich bottom turbid layer becomes the primary route for particle transport within the water column (Hu and Yang 2001).

As discussed above, the average turbidity in the summer is lower than 20 FTU, and the relatively high-turbidity water

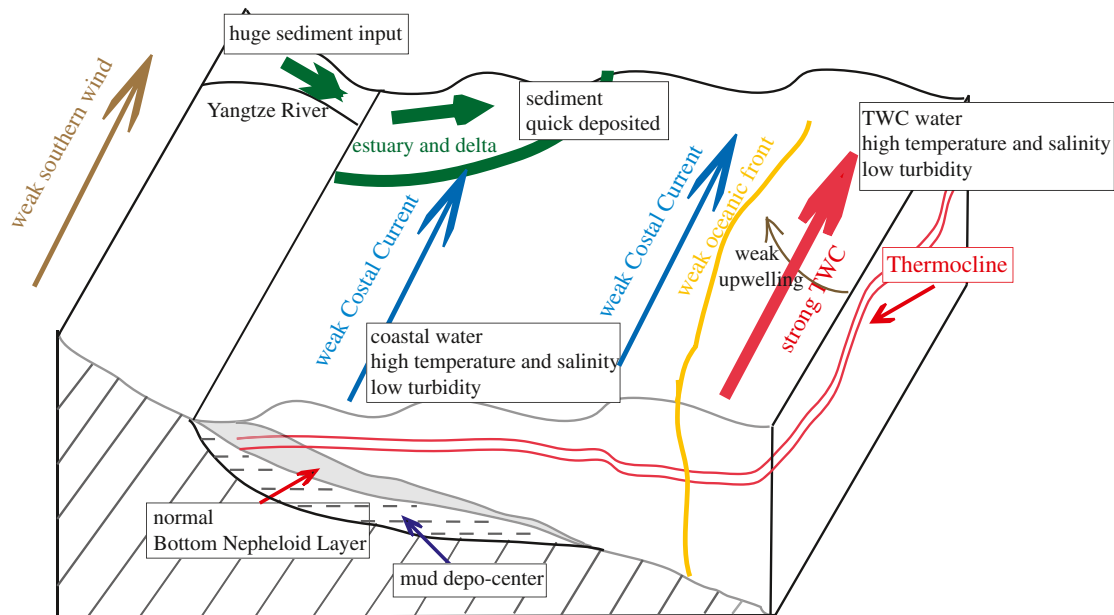
exists only near the shore at the bottom as a thin layer, less than 10 m thick (Figs. 3 and 4). Most of the particles in the bottom turbid layer were derived from the weak resuspension of surface sediments and achieved a neutral buoyancy state. The northward coastal current was relatively weak but the TWC was strong in summer. The distribution pattern of the particles and the hydrodynamic conditions suggested that particle transport was not significant in the summer, especially in the cross-shelf direction, as indicated in previous studies as well (Hu and Yang 2001; Liu et al. 2006). In winter, however, the water turbidities generally increased by several times to more than tenfold, and the expansion of the high-turbidity water was significantly intensified, especially in the cross-shelf direction. Consequently, the particles were partly transported from the northern turbid coastal water and partly originated from the re-suspension of the surface sediments due to the strong winds.

The sediment concentration in the stratum was influenced by the sediment supply and by the dynamical nature of the sedimentary environment. According to the dynamic sedimentary differentiation principle, the deposited sediment might have a substantial difference in grain size, material composition, and geochemical and mineralogical characteristics. The studies on short time scale processes (such as seasonal, annual, and event processes) have important bearings to the geological records in the MDZFC. However, due to the limitations in the observation and sampling techniques, few studies have been conducted so far. The first challenge was to accurately distinguish the differences in the source and dynamic signals. We have attempted to study the seasonal grain size characteristics of the sediment in the MDZFC, and we have interpreted their differences in terms of sedimentary dynamics processes. A significant seasonal variability is found as indicated by the large differences between the surface sediments parameters collected in the two surveys. The ranges of the four main grain size parameters, namely, the median grain size (Mz), standard deviation (SD), skewness (Sk), and kurtosis (Kg), in the samples collected during winter are higher than those collected during summer. However, the Φ values of Mz in the winter samples are generally smaller than those observed in the summer samples. And the gradients of the Sk and Kg are larger than those of the summer samples, for the same station. The variations of the parameters of the surface sediments in this area are mostly attributed to sediment sources and the seasonal differences in the marine environment. The details pertaining to the seasonal variations of the grain size of the surface sediments have been discussed elsewhere (Li et al. 2010).

4.3 Formation mechanism of the MDZFC

Due to the interactions of the coastal water and the TWC, wind, and topography, upwelling occurs at a water depth of

Season 1: in summer



Season 2: in winter

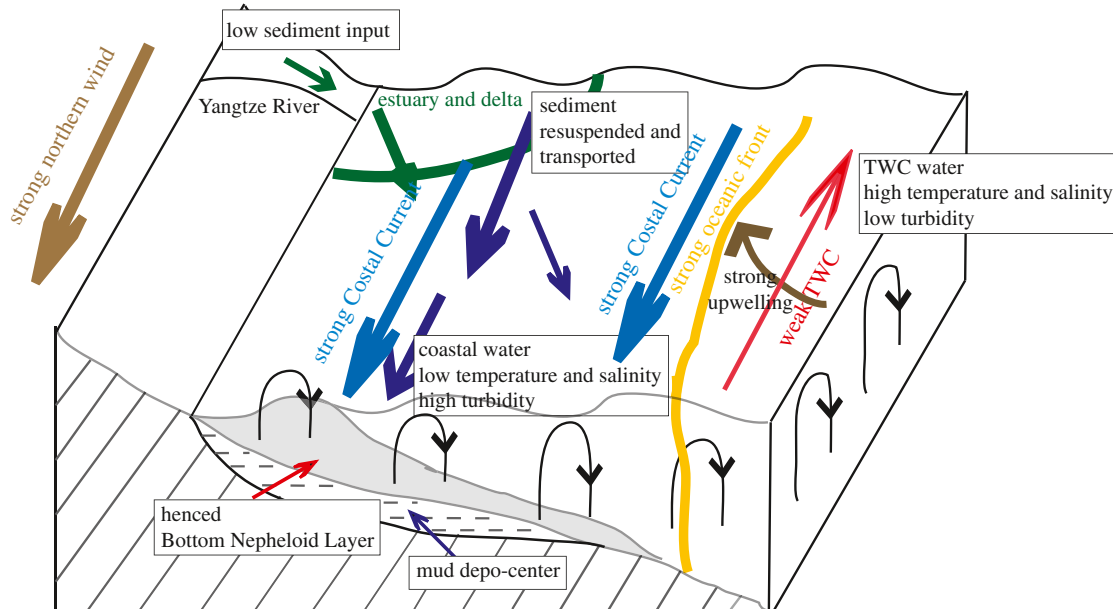


Fig. 8 A conceptual model of the seasonal variations of the water structure and the responsible factors

50 m in the northern MDZFC throughout the year, which appears as a low-temperature and high-salinity water in summer and a high-temperature and high-salinity water in winter (Lv et al. 2006; Qiao et al. 2006). Therefore, an oceanic front develops between the coastal water and the TWC water due to the significant differences in the physical

characteristics and flow directions (Chen 2009), especially during winter (Figs. 3 and 5). Both the upwellings, as well as the oceanic front have significant effects on the formation of the MDZFC. The characteristics of the hydrodynamics and the material supplies suggest that winter is the key season for particle transportation and deposition (Fig. 8).

The water temperature, salinity, and turbidity distributions in winter suggest that the landward diffusion of the high-temperature and high-salinity water occurs in the deep regions at the south and north sides of the study area, whereas the middle part experiences a seaward diffusion of low-temperature and low-salinity coastal water (Fig. 5). In Fig. 5, the sections A and C clearly show the landward diffusion of high-temperature and high-salinity water near the sea bottom, which is absent in section B. The maximum gradients of the temperature and salinity appear between the deep-sea water and coastal water, indicating significant upwelling and front development at the northern and southern parts of the study area, while downwelling occurs in the central area. The high-turbidity water gets distributed primarily in the coastal area, especially in the northern region close to the river estuary. Although the most turbid water is seen in section A, it is limited to only shallow waters without getting diffused into the deep sea. The farthest diffusion front of the turbid water is shown in section B (Fig. 6).

On one hand, the upwelling and oceanic front at the northern and southern regions of the study area prevent the high-turbidity coastal water from diffusing into the deep sea, while on the other hand, it limits the southward flow of the offshore water. The suspended matter does not get deposited in the presence of the strengthened coastal current during winter. Away from the front, the flow gets decelerated and allows most of the particles to be deposited. The downwelling in the middle part of the study area also improves the particle deposition and promotes further diffusion into the deep sea.

5 Conclusions

This study depicts the seasonal variation of the water column structure in terms of temperature, salinity, and turbidity distributions based on field data obtained during the two surveys in the MDZFC. The study analyzes the factors responsible for the seasonal variations in the water column and geological records, and it discusses the sediment transport process and formation mechanism of the MDZFC.

It was found that the water structures in the study area altered significantly with the seasons. In summer, the temperature and salinity of the whole water body were relatively high and markedly stratified with the development of an evident thermocline. In winter, the water body had a relatively low temperature and low salinity and was well mixed from the surface to the bottom. And the water turbidity in winter was much higher in both intensity and extension than in summer. The intruding water crept landward along the sea floor from regions in the sea deeper than 50 m. This water

was more active and stronger in winter, and it exhibited low temperature and high salinity in summer and high temperature and high salinity in winter. The differences in the marine sedimentary environments in the MDZFC were due to the seasonal variations of the hydrodynamic environment, sediment supplies, and circulations. These results suggest that winter is the key season for particle transportation and deposition in the mud depo-center, which is controlled by the upwelling currents and oceanic frontals.

Being devoid of hydrodynamic data, the sediment flux and their seasonal variations could not be calculated in this study. In situ observations gathered using mooring stations are necessary to understand the complete processes of sediment transport and deposition.

Acknowledgments The National Science Foundation of China (grant nos. 40806024, 41276059, and 40976037) and the Scientific Research Foundation of Third Institute of Oceanography, SOA (grant no. TIO2008004) provided the financial support for this work. We would like to acknowledge the assistance provided by the captain and investigators during the fieldwork. This manuscript benefited from comments and suggestions from Andrew James Manning and two anonymous reviewers.

References

- Allison MA, Lee MT, Ogston AS, Aller RC (2000) Origin of Amazon mudbanks along the northeastern coast of South America. *Mar Geol* 163(1–4):241–256. doi:10.1016/S0025-3227(99)00120-6
- Cattaneo A, Correggiari A, Langone L, Trincardi F (2003) The late-Holocene Gargano subaqueous delta, Adriatic shelf: sediment pathways and supply fluctuations. *Mar Geol* 193(1–2):61–91. doi:10.1016/S0025-3227(02)00614-X
- Chen CTA (2009) Chemical and physical fronts in the Bohai, Yellow and East China seas. *J Marine Syst* 78:394–410. doi:10.1016/j.jmarsys.2008.11.016
- DeMaster DJ, McKee BA, Nittrouer CA, Qian JC, Cheng GD (1985) Rates of sediment accumulation and particle reworking based on radiochemical measurements from continental shelf deposits in the East China Sea. *Cont Shelf Res* 4(1–2):143–158. doi:10.1016/0278-4343(85)90026-3
- DeMaster DJ, Kuehl SA, Nittrouer CA (1986) Effects of suspended sediments on geochemical processes near the mouth of the Amazon River: examination of biological silica uptake and the fate of particle-reactive elements. *Cont Shelf Res* 6(1–2):107–125. doi:10.1016/0278-4343(86)90056-7
- Dong LX, Guan WB, Chen Q, Li XH, Liu XH, Zeng XM (2011) Sediment transport in the Yellow Sea and East China Sea. *Estuar Coast Shelf Sci* 93:248–258. doi:10.1016/j.ecss.2011.04.003
- Gong GC, Wen YH, Wang BW, Liu GJ (2003) Seasonal variation of chlorophyll *a* concentration, primary production and environmental conditions in the subtropical East China Sea. *Deep-Sea Res II* 50:1219–1236
- Guo ZG, Yang ZS, Fan DJ, Pan YJ (2003) Seasonal sedimentary effect on the Changjiang estuary mud area. *Acta Geogr Sin* (in Chinese with English abstract) 58(4):591–597

- Hoshika A, Tanimoto T, Mishima Y, Iseki K, Okamura K (2003) Variation of turbidity and particle transport in the bottom layer of the East China Sea. *Deep-Sea Res II* 50(2):443–455. doi:10.1016/S0967-0645(02)00462-9
- Hu DX, Yang ZS (eds) (2001) The key process of marine flux in the East China Sea (in Chinese). Ocean Press, Beijing
- Huh CA, Su CC (1999) Sedimentation dynamics in the East China Sea elucidated from ^{210}Pb , ^{137}Cs and $^{239,240}\text{Pu}$. *Mar Geol* 160(1–2):183–196. doi:10.1016/S0025-3227(99)00020-1
- Kuehl SA, DeMaster DJ, Nittrouer CA (1986) Nature of sediment accumulation on the Amazon continental shelf. *Cont Shelf Res* 6(1–2):209–225. doi:10.1016/0278-4343(86)90061-0
- Kuehl SA, Levy BM, Moore WS, Allison MA (1997) Subaqueous delta of the Ganges–Brahmaputra river system. *Mar Geol* 144(1–3):81–96. doi:10.1016/S0025-3227(97)00075-3
- Li YH, Chen J, Huang CB, Fang JY (2010) Grain-size characteristics of the surface sediments and their seasonal variability in the mud depocenter off the Southern Zhejiang–Fujian Coast. *Acta Sedimentol Sin* (in Chinese with English abstract) 28(1):150–157
- Liu JP, Li AC, Xu KH, Velozzi DM, Yang ZS, Milliman JD, DeMaster DJ (2006) Sedimentary features of the Yangtze River-derived along-shelf clinoform deposit in the East China Sea. *Cont Shelf Res* 26:2141–2156. doi:10.1016/j.csr.2006.07.013
- Liu JP, Xu KH, Li AC, Milliman JD, Velozzi DM, Xiao SB, Yang ZS (2007) Flux and fate of Yangtze River sediment delivered to the East China Sea. *Geomorphology* 85(3–4):208–224. doi:10.1016/j.geomorph.2006.03.023
- Liu JP, Xue Z, Ross K, Wang HJ, Yang ZS, Li AC, Gao S (2009) Fate of sediments delivered to the sea by Asian large rivers: long-distance transport and formation of remote alongshore clinoforms. *The Sedimentary Record* 7(4):4–9
- Liu SF, Shi XF, Liu YG, Qiao SQ, Yang G, Fang XS, Wu YH, Li CX, Li XY, Zhu AM, Gao JJ (2010) Records of the East Asian winter monsoon from the mud area on the inner shelf of the East China Sea since the mid-Holocene. *Chin Sci Bull* 55(21):2306–2314. doi:10.1007/s11434-010-3215-3
- Liu SF, Shi XF, Liu YG, Wu YH, Qiao SQ, Yang G (2011) Recent 2000 a climatic record of mud area on the inner shelf of the East China Sea. *Acta Oceanol Sin* 33(3):85–93
- Lv XG, Qiao FL, Xia CS, Zhu JR, Yuan YL (2006) Upwelling off Yangtze River estuary in summer. *J Geophys Res* 111, C11S08, doi:10.1029/2005JC003250
- McKee BA, Nittrouer CA, DeMaster DJ (1983) Concepts of sediment deposition and accumulation applied to the continental shelf near the mouth of the Yangtze River. *Geology* 11(11):631–633
- McKee BA, Aller RC, Allison MA, Bianchi TS, Kineke GC (2004) Transport and transformation of dissolved and particulate materials on continental margins influenced by major rivers: benthic boundary layer and seabed processes. *Cont Shelf Res* 24(7–8):899–926. doi:10.1016/j.csr.2004.02.009
- Milliman JD, Shen HT, Yang ZS, Meade RH (1985) Transport and deposition of river sediment in the Changjiang estuary and adjacent continental shelf. *Cont Shelf Res* 4(1–2):37–45. doi:10.1016/0278-4343(85)90020-2
- Qiao FL, Yang YZ, Lv XG, Xia CS, Chen XY, Wang BD, Yuan YL (2006) Coastal upwelling in the East China Sea in winter. *J Geophys Res* 111, C11S06, doi:10.1029/2005JC003264
- Su CC, Huh CA (2002) ^{210}Pb , ^{137}Cs and $^{239,240}\text{Pu}$ in East China Sea sediments: sources, pathways and budgets of sediments and radionuclides. *Mar Geol* 183(1–4):163–178. doi:10.1016/S0025-3227(02)00165-2
- Su JL (ed) (2005) The oceanography in the Chinese margin sea. Ocean Press, Beijing (in Chinese)
- Xu KH, Milliman JD (2009) Seasonal variations of sediment discharge from the Yangtze River before and after impoundment of the Three Gorges Dam. *Geomorphology* 104:276–283
- Xu KH, Milliman JD, Li AC, Liu JP, Kao SJ, Wan SM (2009) Yangtze- and Taiwan-derived sediments on the inner shelf of East China Sea. *Cont Shelf Res* 29(18):2240–2256. doi:10.1016/j.csr.2009.08.017
- Xu KH, Li AC, Liu JP, Milliman JD, Yang ZS, Kao SJ, Wan SM, Xu FJ (2012) Provenance, structure, and formation of the mud wedge along inner continental shelf of the East China Sea: a synthesis of the Yangtze dispersal system. *Mar Geol* 291–294(1):176–191. doi:10.1016/j.margeo.2011.06.003
- Yang ZS, Guo ZG, Wang ZX, Xu JP, Gao WB (1992) Basic pattern of transport of suspended matter from the Yellow Sea and East China Sea to the eastern deep seas. *Acta Oceanol Sin* (in Chinese with English abstract) 14(2):81–90
- Zhu J (2003) Dynamic mechanism of the upwelling on the west side of the submerged river valley off the Changjiang mouth in summer-time. *Chin Sci Bull* 48(24):2754–2758